

Improved Research on the Transformer-Inductor Simulation Model of Magnetics

Jiang Liyuan, Liu Baoyuan, Zhang Li

Beijing Jiaotong University Haibin College, Hebei 061100, China

Abstract: Transformer-inductor simulation model not only reflects the characteristics of magnetic path and circuit, but also brings in magnetic components that reflected the parasitic capacitance. There are further research, strict derivation and magnetic circuit equivalent for the model in this article. Under the condition of considering hysteresis, saturation effect we can conclude a new modeling and its equivalent, which can make the magnetic curve and characteristic get better fitting. It shows that the transformer-inductance simulation model is easy to spread and use.

Key words: Mcomponents; Simulation model; Nonlinear; Hysteresis B-H curve

Published online: 30th Nov 2017

Corresponding author: Jiang Liyuan, E-mail: 595361588@qq.com

1 Introduction

At present, based on the magnetic dual circuit method, the mathematical model of magnetic device can be divided into two categories: magnetic circuit-dual circuit equivalent model and gyroscope-capacitance equivalent circuit model. In the two models, the former cannot reflect the magnetic path parameters, and the latter can reflect the electric circuit and the magnetic circuit characteristics of magnetic component, but because it is a magnetic guide with capacitive simulation, it is easy to be confused with the concept of the stray capacitance of capacitance simulation in high frequency. In this paper, a new model -

transformer-inductance simulation model (T-I model) is studied, and this model not only utilizes the magnetic circuit-dual circuit transform method, which can fully and clearly reflect the magnetic circuit of magnetic component and the magnetic circuit characteristics, but also the parameters that reflect the parasitic effect can be conveniently joined. In this paper, the magnetic dual circuit method is adopted to conduct modeling and theory conclusion on the simulation of the magnetic hysteresis effect of magnetic component and saturation effect on T-I model. [1]

2 The Improved T-I Model of Magnetic Component

2.1 The Improved T-I Model of Magnetic Component

The Figure 1 is the improved T-I model. According to the magnetic circuit-dual circuit analogous relation, the magnetic potential in the magnetic component can be compared with partial electric current of magnetic circuit in the model, and the magnetic conductance of magnetic component can be compared with the partial nonlinear resistance of magnetic circuit in the model. The characteristics of magnetic hysteresis in the model are simulated by the series connection (getting nonlinear resistance) of the fixed resistance R and the controlled voltage source. Nonlinear characteristics are simulated by the parallel connection of the fixed inductance L and controlled current source; Saturation characteristics are simulated by the parallel connection of the fixed conductance G and controlled current source. [2]

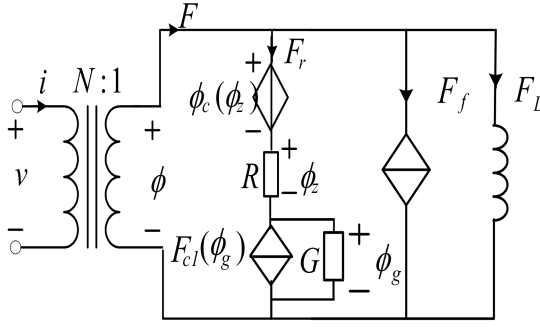


Figure 1 Improved T-I model

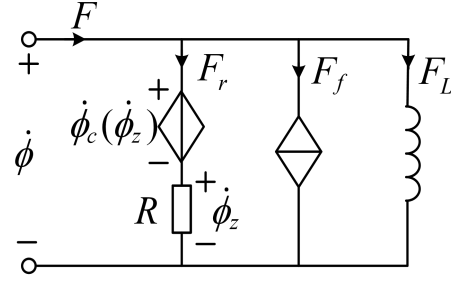


Figure 2 T-I model by nonlinear resistance

2.1.1 Nonlinear Inductance T-I Model Considering Magnetic Hysteresis

On the simulation of the characteristics of magnetic hysteresis of magnetic component, nonlinear controlled voltage source (by $\dot{\phi}_z$ control) $\dot{\phi}_c$ and R the series connection are led in the model for the purpose of reducing the influence of excitation source size on the hysteresis loop width, as shown in Figure 2^[3-5].

The functional equation of controlled voltage source is shown in the following formula, which is the result of the simplified equation in reference^[6].

$$\dot{\phi}_c(\dot{\phi}_z) = c(\dot{\phi}_z)^m = c(RF_r)^m \quad (1)$$

When the hysteresis property is considered only, the following relation can be obtained from Figure 2.

$$\dot{\phi} = c(RF_r)^m + RF_r \quad (2)$$

Therefore, the equivalent nonlinear resistance obtaining F_r branch can be worked out:

$$R_{eq} = \dot{\phi}/F_r = cR^m F_r^{m-1} + R \quad (3)$$

Simulating characteristics of magnetic hysteresis of the magnetic component by resistance conforms to the physical mechanism. Because the resistance voltage $\dot{\phi}_z$ and $\dot{\phi}$ meet the relative reference direction, the partial pressure of the resistance will hinder the change of the flux, which is shown as the magnetic hysteresis characteristic.

2.1.2 Nonlinear Inductance T-I Model Considering Magnetic Saturation

On the verification of the saturation characteristics of the model, the change of incentive magnetic potential F_s is random, so the nonlinear controlled current source F_{cl} controlled by $\dot{\phi}_g$ (different from F_ϕ) and the conductance G parallel are stimulated in this paper, as shown in Figure 3.^[6]

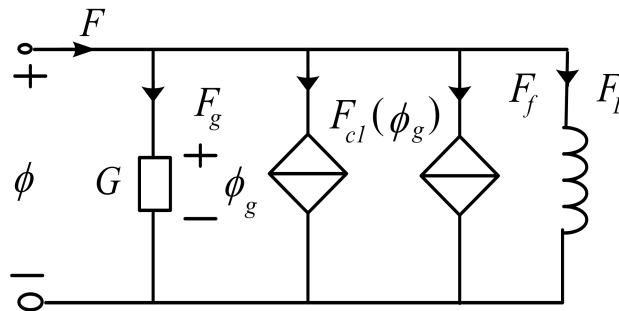


Figure 3 T-I model by nonlinear conductivity

The nonlinear controlled current source can be described in the following formula:

$$F_{c1}(\dot{\phi}_g) = \lambda(\dot{\phi}_g)^n = \lambda(F_g/G)^n \quad (4)$$

The following relation can be obtained from Figure 3:

$$F_G = \lambda(F_g/G)^n + F_g \quad (5)$$

So the equivalent nonlinear conductance of F_G branch is

$$G_{eq} = F_G/\dot{\phi} = \lambda(F_g/G)^{n-1} + G \quad (6)$$

When the voltage value of the both ends of the conductance G is less and the flux is less, the controlled current source is correspondingly small, and the magnetic potential is almost always on the conductance G , so the equivalent magnetic guide is G_{eq} . Naturally, when the voltage value of the both ends of the conductance is more and the flux is more, the figure of $F_{c1}(\dot{\phi}_g)$ will increase exponentially. Because the magnetic potential is mainly provided by the controlled source, if the $\dot{\phi}$ is approximately zero, the magnetic component is at the saturation state.

3 The Calculation of the Parameters in the Model

The input parameters of the model can be divided into two types: the material parameters and geometric parameters of magnetic core. The material parameters include saturation magnetic flux density B_{sat} , saturation magnetic field intensity H_{sat} , residual flux density B_r , coercive force H_c , relative permeability $B-H$ of linear segments of curve, μ_r curve and $B-H$ so on. And the geometrical parameters include the area A_e of the effective magnetic circuit, and the length l_e of the effective magnetic circuit. The following parameters are used to conduct the model parameters, which include the parameter influencing magnetic hysteresis characteristics R , c , m and the parameter influencing the saturation characteristics G , λ , n .^[6]

3.1 The Simulation of Input Parameters

As mentioned above, a nonlinear controlled current source F_f is used to simulate the nonlinear characteristics of the magnetic component model. The b_i ($i=3,5,7,\dots$) of can adopt the calculation method of data fitting. Within a certain range of precision, the formula can be simplified to the formula (7), and that is, a certain higher term is solely used to simulate the nonlinear of magnetic core. Namely,

$$F = a_1 f + b_n a_1^n f^n \quad (7)$$

The practical simulation of this controlled source will be discussed below to show that there is little difference using formula (7) to conduct the simplified analysis. According to the magnetization curve standard in the magnetic core manual, the formula (7) is converted to the relational formula, between H and B which is as follows:

$$H = \frac{a_1 A_e}{l_e} B + \frac{b_n a_1^n A_e^n}{l_e} B^n \quad (8)$$

In the formula, A_e is the effective magnetic conductive area and the l_e is the effective magnetic circuit length.^[3]

3.2 The Conclusion of Magnetic Hysteresis Parameters

Because the $\dot{\phi}$ and F follow the circuit theory in the model, the equation and the solving differential equation among the $\dot{\phi}$ and each branch F can be listed drawing on Ampere's rule, the relationship between ϕ and F can be worked out, and the magnetic hysteresis parameters can be calculated by combining with the points (B_1, H_1) , (B_s, H_s) , the corresponding (ϕ_1, F_1) , and (ϕ_s, F_s) , of the fundamental magnetization curve.

3.2.1 Calculation R

From the Figure 4 simulating inductance magnetic hysteresis effect:

$$F = F_r + F_f + F_L \quad (9)$$

Namely,

$$F = F_r + a_1 f + b_n a_1^n f^n \quad (10)$$

When the magnetic core is unsaturated, it satisfies the following formula:

$$F_r = \dot{\phi}/R \quad (11)$$

Without loss of generality, has $F = F_s \sin \omega t$

$$\dot{\phi}/R + a_1 \phi + b_n a_1^n \phi^n = F_s \sin \omega t \quad (12)$$

Because the non-odd nonlinear differential equation solving is trivial, the numerical value ϕ is not easy to obtain, and it's also because when the hysteresis effect is simulated, the main parameters are the remanence B_r (corresponding ϕ_r) and the coercive force H_c (corresponding F_c), and at the same time, because the higher power of the nonlinear equation is very small in the vicinity of zero, it can be approximately believed ϕ_r and F_c is only influenced by $F_L = a_1 f$ when the hysteresis effect is simulated. Therefore, the expression can be obtained:

$$\dot{\phi}/R + a_1 \phi = F_s \sin \omega t \quad (13)$$

Solve the differential equation, and the result is shown in equation (14):

$$\phi = \frac{RF_s(a_1 R \sin \omega t - \omega \cos \omega t)}{a_1^2 R^2 + \omega^2} \quad (14)$$

Therefore, the magnetic potential F and flux ϕ have established a parametric equation with the parameter t , and if t is removed, the equation expressing the relationship between F and ϕ can be obtained

$$\frac{(a_1 R^2 F - a_1^2 R^2 \phi - \omega^2 \phi)^2}{\omega^2 R^2 F_s^2} + \frac{F^2}{F_s^2} = 1 \quad (15)$$

Substitute equation (13):

$$F_r = F_s \sin \omega t - a_1 \phi \quad (16)$$

The following equation can be obtained by removing the intermediate variable t from equation (14) and equation (22)

$$\frac{(a_1 R^2 F_r - \omega^2 \phi)^2}{\omega^2 R^2 F_s^2} + \frac{(F_r + a_1 \phi)^2}{F_s^2} = 1 \quad (17)$$

Then, the equivalent nonlinear resistance R_{eq} in the branch is used to replace R in equation (17) and the value of R is determined by $F_r(\phi = \phi_s) = 0$.

$$R = \omega \phi_s / \sqrt{F_s^2 - a_1^2 \phi_s^2} \quad (18)$$

3.2.2 Select m

As can be seen from equation (3), the three parameters of R , c and m all influence the value of F_c . To ensure that the value of R_{eq} is not negative, the value of m shall be the odd number. From the above analysis, as m increases, the impact of stimulated magnetic hysteresis of magnetic pieces will be smaller, so the selection of m shall be as large as possible.^[5]

3.2.3 Calculate c

Replace R in equation (17) with the equivalent nonlinear resistance R_{eq} of F_r , and the value of c is determined through $F_r|_{\phi=0} = F_c$.

$$c = \frac{\omega \sqrt{\omega^2 \phi_s^2 + a_1^2 R^2 \phi_s^2 - R^2 F_c^2} - R}{a_1 R^{m+1} F_c^m} \quad (19)$$

3.3 Calculation of Parameters of Saturation

3.3.1 Calculation of G

The following magnetic potential relationship can be deduced from the introduction of the nonlinear conductance T-I model (Figure 3):

$$F = F_G + F_f + F_L \quad (20)$$

Among them, F_G represents the sum of the current flowing by the conductance and the controlled current source in parallel therewith. If linear conductance is used for simulation calculation, then

$$\dot{\phi}G + a_1 \phi = F_s \sin \omega t \quad (21)$$

Equation (21) is a differential equation, and the following can be obtained by solving it:

$$\phi = \left(\frac{a_1}{G} \sin \omega t - \omega \cos \omega t \right) \times G \times \frac{F_s}{a_1^2 + \omega^2 G^2} \quad (22)$$

Magnetic potential F and ϕ constitute a set of parametric equations

$$\begin{cases} F = F_s \sin \omega t \\ \phi = \left(\frac{a_1}{G} \sin \omega t - \omega \cos \omega t \right) \times G \times \frac{F_s}{a_1^2 + \omega^2 G^2} \end{cases} \quad (23)$$

The following can be obtained by eliminating the parameter t from the above equation

$$\left[\frac{a_1(F_g + a_1\phi)}{GF_s} - \frac{\phi(a_1 + \omega^2 G^2)}{GF_s} \right]^2 \times \frac{1}{\omega^2} + \frac{(F_g + a_1\phi)^2}{F_s^2} = 1 \quad (24)$$

The following can be obtained from $F_G(\phi = \phi_s) = 0$

$$G = a_1 F_g / \omega \sqrt{F_s^2 - F_g^2} \quad (25)$$

3.3.2 Selection of n

As can be seen from equation (6), as flux increases, $F_{cl}(\dot{\phi}_g)$ increases exponentially, and when reaching a certain degree, the magnetic potential will mainly fall on the controlled source, while the magnetic pieces will be saturated. From calculation, we can see that to ensure that the value of G_{eq} is non-negative, n shall take the odd number.^[7]

3.3.3 Calculation of λ

Use the equivalent nonlinear resistance G_{eq} of F_G branch to replace G in equation (23), and the value of λ can be calculated from $F_G|_{F=0} = F_g$. Therefore

$$F_g = \pm \omega F_s / \sqrt{a_1^2 + \frac{\omega^2}{(\lambda \frac{F_g}{G^{n-1}} + G)^2}} \quad (26)$$

The expression of parameter c can be obtained from equation (26)

$$\lambda = \left(\frac{\omega F_{cl}}{\sqrt{\omega^2 F_s^2 - a_1^2 F_{cl}^2}} - G \right) \times \frac{G^{n-1}}{F_{cl}^{n-1}} \quad (27)$$

4 Simulation Realization and Results of the Model

4.1 Simulation of Nonlinear Inductance Model

Use the relationship between magnetic field intensity H and magnetic induction intensity B in the above equation (8) to carry out theoretical simulation. To facilitate analysis, take effective magnetic conductivity area $A_e = 1 \text{ m}^2$ (corresponding to $m_e = 2000$),

$b_n = 3.2 \times 10^{-9}$ (here, b_n is a given value) to conduct quantitative analysis, and the basic magnetic curve is shown in Figure 4 (a).^[8]

Using the equivalent circuit in Figure 3 to simulate, and analog parameters are set as follows: $F(t) = 500 \sin(314t) \text{ A}$, $L_1 = 2.513 \text{ mH}$. The basic magnetic curve obtained by model analog is shown in Figure 4 (b), showing that analog results are consistent with the theoretical analysis.

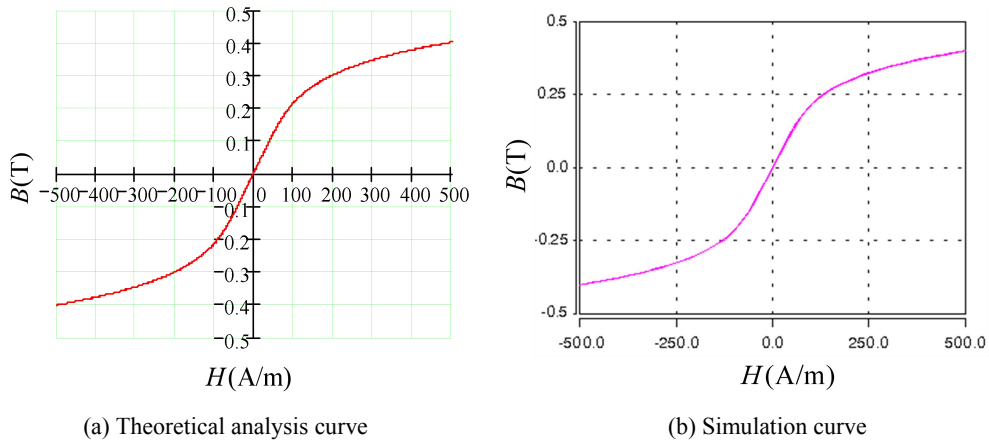


Figure 4 Basic magnetic properties of simulation

4.2 Hysteresis Model Simulation

The selected simulation parameters are as follows: $\phi = 0.4\text{Wb}$, $F_s = 500\text{A}$, $F_c = 20$, $m = 7$ and other parameters are the same as before. Through calculation, it can be obtained that resistance $R = 0.265\Omega$, $c = 3.356 \times 10^{-3}$ and values of amplitude of excitation F are 500, 750 and 1000. The hysteresis effect using nonlinear resistance simulation and the results corresponding to the analog hysteresis curve are shown in Figure 5. It can be seen from the figure that, with the introduction of the T-I model of non-linear resistance, the simulation

coercivity F_c and residual magnetism ϕ_r will not be greatly

affected by F_m .^[9]

Different F_c are given, the value of c will be calculated according to equation (19) for simulation according to the calculated c and simulation results are shown in Table 1. By comparing theoretical and analog values, it can be seen that the analog forward magnetic value is slightly larger than the theoretical value while the reverse magnetic value is slightly smaller than the theoretical value. Therefore, it can be proved that analog results are basically consistent with the theoretical analysis results. Therefore, parameter c can be fully determined by using equation (19).

Table 1 Comparison between theoretical and simulation value of F_c under various parameter c

Given F_c	Calculated C	Simulated F_c
10	0.429	-9.925
20		-19.981
30	1.962×10^{-4}	-29.932
40	2.615×10^{-5}	-39.954
50	5.475×10^{-6}	-49.915
60	1.524×10^{-6}	-59.931
70	5.169×10^{-7}	-69.971

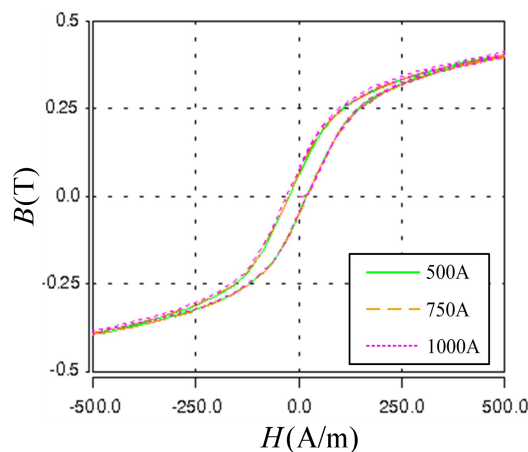


Figure 5 Simulation hysteresis curves under various excitations

Another important parameter that reflects the characteristic of the hysteresis loop is the residual

magnetism B_r (i.e. the corresponding ϕ_r). With further

analysis of the synthetic hysteresis curve and in terms of non-rectangular magnetic materials, the parameter a_1 can be determined by the following equation

$$a_1 = F_c / \phi_r \quad (28)$$

As for rectangular hysteresis material, as the magnetic permeability is very large, it can be directly determined according to μ

$$a_1 = l_e / \mu_e \mu_0 A_e \quad (29)$$

By referring to the $B-H$ curve in the magnetic core data manual, turning points exist from the linear to saturation segments. Select a value of magnetic flux density B_1 at turning points, which corresponds to two magnetic field intensity H_{\min} and H_{\max} , and the average value H_1 of the two are taken as the magnetic field intensity in the basic magnetic curve, therefore

$$H_1 = (H_{\min} + H_{\max}) / 2 \quad (30)$$

B_1 and H_1 are equivalent to ϕ_1 and F_1 , which will be substituted into equation (7) along with ϕ_s and F_s to

obtain values of parameters n and b_n .

$$\begin{cases} n = \frac{\ln(F_s - a_1 \phi_s) - \ln(F_1 - a_1 \phi_1)}{\ln \phi_s - \ln \phi_1} \\ b_n = \frac{F_s - a_1 \phi_s}{a_1^n \phi_s^n} \end{cases} \quad (31)$$

4.3 Characteristic of Saturation Simulation

By referring to the magnetic core manual, use the slope ϕ and F corresponding to variables of the $B-H$ curve to simulate the characteristic of saturation. During calculation, the taken parameters are the same as before, take the derivative of the parameter F in equation (23), and the following can be obtained

$$\frac{d\phi}{dF} = \left(\frac{a_1}{G} \pm \frac{\omega F}{\sqrt{F_s^2 - F^2}} \right) \times \frac{G}{a_1^2 + \omega^2 G^2} \quad (32)$$

Set the above equation $d\phi/dF = 0$, and saturated magnetic potential F_{sat} and magnetic induction intensity H_{sat} can be obtained.

$$\begin{cases} \phi_{sat} = \left(\pm \frac{\omega^3 G^3 F_s^2}{a_1^2 + G^2 \omega^2} \pm \frac{F_s a_1^2}{\sqrt{a_1^2 + G^2 \omega^2}} \right) / (a_1^2 + G^2 \omega^2) \\ F_{sat} = \pm \frac{F_s a_1}{\sqrt{a_1^2 + G^2 \omega^2}} \end{cases}$$

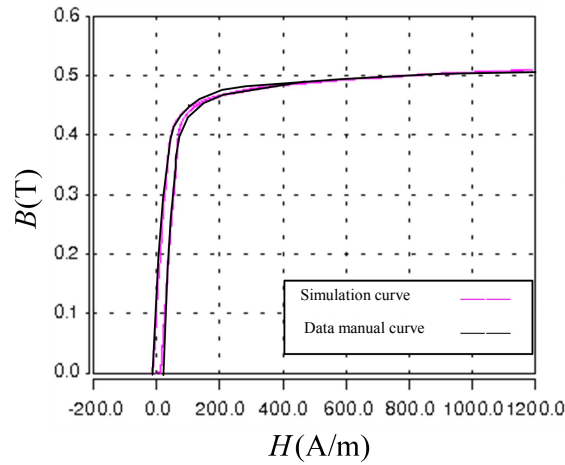


Figure 6 Simulation of saturation model

In equation (33), $\pm F_s a_1^2 / \sqrt{a_1^2 + G^2 \omega^2}$ is much smaller than the previous value, which can be omitted in calculation. Calculated values of the saturated magnetic potential and saturated magnetic induction intensity can be deduced, and it can be seen that theoretical and calculated values are very close.^[10]

$$\begin{cases} \phi_{sat} = 0.5(\text{NegativeRounding}) \\ F_{sat} = \pm 497.6 \end{cases} \quad (34)$$

When verifying, the equation can be regarded as the quadratic equation with G as the unknown element.

$$\frac{d\phi}{dF}\omega^2G^2 \pm \frac{\omega F}{\sqrt{F_s^2 - F^2}}G + \frac{d\phi}{dF}a_1^2 - a_1 = 0 \quad (35)$$

As $G \neq 0$, it can be known that in the equation, $\geq \Delta 0$, and the corresponding relationship between $d\phi/dF$ and F can be obtained.

$$\Delta = \frac{\omega^2 F^2}{F_s^2 - F^2} - 4 \frac{d\phi}{dF} \omega^2 \left(\frac{d\phi}{dF} a_1^2 - a_1 \right) \geq 0 \quad (36)$$

Set $\Delta = 0$, and in this situation, G has the unique answer,

and the $d\phi/dF$ expression can be obtained.

$$\frac{d\phi}{dF} = 1 \pm \sqrt{1 - \frac{F^2}{F_s^2 - F^2}} / 2a_1 \quad (37)$$

$$\frac{d\phi}{dF} = \frac{-(0.2 \times 10^{-4} F^2 + 5) \pm \sqrt{3 \times 10^{-4} F^2 + 5^2}}{0.4 \times 399 \times 10^{-4} F^2 - 3990} \quad (38)$$

By using the above parameters of $a_1 = 399$ and $F_s = 500$, $G = 0.387$, so $d\phi/dF$ and F can be obtained. Compared it with curve values in the magnetic core data manual to prove that this model is practical and applicable.^[11]

Table 2 Comparison between theoretical and simulation value of $d\phi/dF$ under various parameter F

F theoretical value	100	125	150	200
$d\phi/dF$ theoretical value	0.002739	0.002877	0.003053	0.003545
ϕ theoretical value	0.3969	0.4189	0.4398	0.4653
F manual value	100	125	150	200
$d\phi/dF$ manual value	0.00137	0.000974	0.000707	0.0002969
ϕ manual value	0.4	0.428	0.45	0.475

5 Conclusion

The experimental platform is a four-phase (two-phase high) VRM test platform, its control chip is ISL6558EVAL1Z, the input voltage is 12VDC, the output voltage is 1.5VDC, the control chip is ISL6558, and the switch tube MOSFET selects HUF76143S3S; the inductance of the integrated magnet pieces is $L1 = 100.4\mu H$ and $L2 = 101.2\mu H$; the

iron core selects spiral film magnetic pieces, and its winding air gap is $g_c = 0.4mm$; the amount of leakage inductance is about $41.2\mu H$. After verification, several results in the following figures can be obtained. The Figure 7 is the trigger waveform of switch tube, Figure 8 is the inductance current of single channel, Figure 9 is the current waveform of two-phase inductance and Figure 10 is the total output current.^[12]

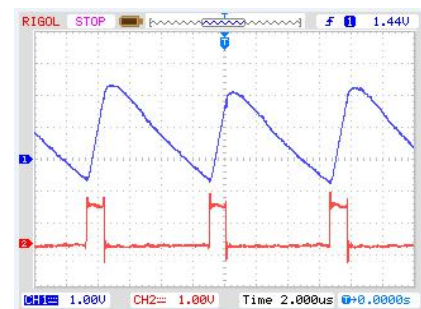


Figure 7 The trigger waveform of switch tube Figure 8 The inductance current of single channel



Figure 9 The current waveform of two-phase inductance

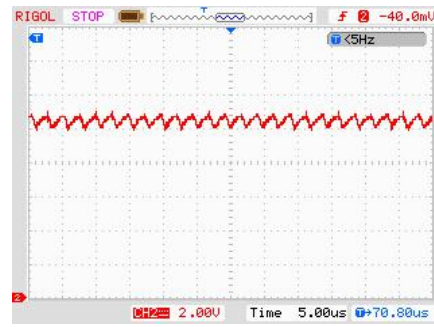


Figure 10 The total output current

6 Concluding Remarks

In this article, a new T-I simulation model of magnetic pieces is deduced theoretically, which solves the problem that effect degree of the excitation on the width of hysteresis curve when the linear resistance simulates hysteresis. At the same time, the methods of determining the model and its parameters are given. The B-H simulation curve is obtained by giving certain excitation and material parameters, and be compared with the data manual curve. The results show the accuracy of the model and model parameters.

References

- [1] Zengyi Lu, Wei Chen. Multi-Phase Inductor Coupling Scheme with Balancing Winding in VRM Applications[C]. Proc. IEEE APEC, 2007:731-735
- [2] Qianhong Chen, Yang Feng, Linqun Zhou, et.al.. Active Clamp Positive Excitation Integrated Converter with Minimized Output Ripple[J]. Proceedings of the CSEE, 2009,(03).
- [3] Hongzhu Li, Liyuan Jiang, Wei Jia, et.al. Research on the transformer-inductor simulation model of magnetics[J]. Journal of Power Sources Technology, 2011, 11-12.
- [4] Cheng D K, Wong L, Lee Y S. Design, Modeling, and Analysis of Integrated Magnetics for Power Converters[C]. IEEE Power Electronics Specialists Conference, 2000,1:320-325.
- [5] Liyuan Jiang. Research on the Equivalent Circuit Model of Thin Film Magnetic Component Under the

Magnetic Integration Technology[D]. Liaoning: Liaoning Technical University, 2012.

- [6] Yugang Yang, Hongzhu Li, Jianlin Wang, et.al. Application of Integrated Magnetic Pieces Whose DC-bias can be Reduced in DC/DC Converter[J]. Proceedings of the CSEE, 2005,25(11):50-54.
- [7] Qianhong Chen, Ligang Xu, Zhuyun Li, et.al. Improved Gyroscope-Capacitance Nonlinear Magnetic Core Simulation Model[J]. Transactions of China Electrotechnical Society, 2009,24(4): 14-21.
- [8]Liang Yan, Brad Lehman, Better. Understanding and Synthesis of Integrated Magnetics with Simplified Gyrator Model Method[J]. Canada, IEEE-PESC, Vancouver, British Columbia, 2001:433-438
- [9] R.T. Chen, Y.Y. Chen. Synthesis and Design of Integrated-Magnetic-Circuit Transformer for VRM Application[J]. IEE Proc.-Electr. Power Appl. 2006,53(3): 369-378
- [10] Wong L P, Lee Y S, Cheng D K. A New Approach to the Analysis and Design of Integrated Magnetics[C]. IEEE Power Electronics Specialists Conference, 2001:1196-1202.
- [11] Jieli Li, Anthony Stratakos, Aaron Schultz, et.al. Using Coupled Inductors to Enhance Transient Performance of Multi-Phase Buck Converters[C]. Proc. IEEE APEC, 2004:1289-1293
- [12] Yong Zhou, Zhimin Zhou, Ying Cao. Fabrication and Performance of Fe-Based Magnetic Thin Film Inductor for High-Frequency Application. Journal of Magnetism and Magnetic Materials, 2008.4